Excitation Function for the Production of ^{262}Bh (Z = 107) in the Odd-Z-Projectile Reaction ^{208}Pb(^{55}Mn, n)

C. M. Folden III,[1,2] S. L. Nelson,[1,2] Ch. E. Düllmann,[1,2] J. M. Schwantes,[1,2] R. Sudowe,[1] P. M. Zielinski,[1,2] K. E. Gregorich,[1] H. Nitsche,[1,2] and D. C. Hoffman[1,2]

[1] Nuclear Science Division, Lawrence Berkeley National Laboratory, Berkeley, California 94720

[2] Department of Chemistry, University of California, Berkeley, California 94720

ABSTRACT

The excitation function for production of ^{262}Bh in the odd-Z-projectile reaction ^{208}Pb(^{55}Mn, n) has been measured at three projectile energies using the Berkeley Gas-filled Separator at the Lawrence Berkeley National Laboratory 88-Inch Cyclotron. In total, 33 decay chains originating from ^{262}Bh and 2 decay chains originating from ^{261}Bh were observed. The measured decay properties are in good agreement with previous reports. The maximum cross section of 540^{+180}_{-150} pb is observed at a lab-frame center-of-target energy of 264.0 MeV and is more than fives times larger than that expected based on previously reported results for production of ^{262}Bh in the analogous even-Z-projectile reaction ^{209}Bi(^{54}Cr, n). Our results indicate that the optimum beam energy in one-neutron-out heavy-ion fusion reactions can be estimated simply using the "Optimum Energy Rule" proposed by Świątecki, Siwek-Wilczyńska, and Wilczyński.

PACS numbers: 25.70.-z, 25.70.Gh, 23.60.+e, 27.90.+b

I. INTRODUCTION

"Cold" nuclear fusion reactions have been successfully employed in the production of transactinide elements, most notably in the discovery of elements 107-111 (see [1-2] for reviews) and reports of the production of elements 112 [3-4] and 113 [5]. The ^{55}Mn + ^{208}Pb reaction was studied for the first time by Oganessian *et al*. [6-7] using a rotating drum system. A new spontaneous fission (SF) activity with half-life ≈ 1-2 ms and ≈ 20% SF branch was reported and assigned to ^{261}Bh (bohrium, Z = 107), the 2n product of complete fusion. Later experiments [8] focused on SF decay of the 1n product ^{262}Bh and also added periodic radiochemical separations to search for the presumed long-lived daughter ^{246}Cf ($t_{½}$ = 35.7 h [9]). ^{246}Cf would be formed if ^{262}Bh undergoes the probable decay scheme of four total alpha decays and an electron-capture (EC) decay. Although ^{246}Cf was detected in the Cf fractions, many assumptions were required to assert that it is produced as a result of the decay of ^{262}Bh. These results were not confirmed and the first definitive evidence for the production of bohrium was reported by Münzenberg *et al*. [10-11]. They reported that ^{262}Bh decays from the ground state by emission of alpha groups of several different energies and a half-life of 102 ± 26 ms based on the observed distribution of lifetimes. An alpha-decaying isomeric state was also reported with a half-life of 8.0 ± 2.1 ms. Additionally, they reported the discovery of ^{261}Bh, which decays with a half-life of $11.8^{+5.3}_{-2.8}$ ms by the emission of alpha-particles. Münzenberg *et al*. were unable to confirm the reports of decay by SF for either nuclide. These reports were strengthened by the observation of genetically linked alpha-decay chains which could be followed to the decay of the known nuclides ^{250}Fm and ^{250}Md. Subsequent experiments [12-14] showed that ^{262}Bh was produced as the alpha-decay product of ^{266}Mt (Z = 109) and the same decay properties were observed. In

light of the results reported by Münzenberg *et al.*, the odd-*Z*-projectile ^{208}Pb(^{55}Mn, *n*) reaction for the production of ^{262}Bh has been re-examined using modern techniques and instrumentation.

II. EXPERIMENTS

Experiments were conducted at the Lawrence Berkeley National Laboratory (LBNL) 88-Inch Cyclotron using the Berkeley Gas-filled Separator (BGS). The BGS has been described in [15-16] and recent improvements are given in [17-18]. The focal plane detector consists of 48 vertically position-sensitive strips with an active area 178-mm wide by 58-mm high. These strips are numbered so that particles with high magnetic rigidity implant in strip 0 and those with low magnetic rigidity implant in strip 47. Horizontal positions are determined by the strip number and vertical positions from -29 mm to +29 mm are determined by resistive charge division. Thirty-two additional "upstream" detectors are mounted perpendicular to the face of the main strip detectors to form a five-sided box configuration. An implantation event or radioactive decay depositing more than $\approx$ 300 keV in any of these detectors triggers the Multi-Branch System [19-20] list-mode data acquisition system. Signals from each end of a strip detector are processed by an amplifier with two different output ranges: a "low-energy" range to maximize energy resolution of alphalike events, and a "high-energy" range to ensure a sufficient maximum energy for detecting SF events. Implantation events could fall into either range depending on energy. Detectors were calibrated using external alpha-particle sources of ^{148}Gd, ^{239}Pu, ^{241}Am, and ^{244}Cm, and the implanted alpha-decaying products of the ^{133}Cs(^{55}Mn, *xn*)$^{188-x}$Hg, x = 3-5 and ^{127}I(^{55}Mn, *yn*)$^{182-y}$Pt, y = 3-5 reactions using a CsI target. ^{211}Po^{g} produced in transfer reactions with the ^{208}Pb targets was also used as a calibration standard. High-energy calibrations were extrapolated from the low-energy calibrations. An additional set of twelve uncalibrated "punch through" detectors covering the entire width of the

focal plane was mounted behind the strip detectors to provide a veto for light, low-ionizing particles which traversed the separator. All detectors consist of 300-μm-thick Si mounted on 0.15-μm-thick Al. These detectors were not sensitive to electron-capture (EC) decay but the observation of alpha decay of the EC daughter would indicate that the previous EC had occurred. The standard deviation of the energy of alpha particles fully stopped in the strip detectors was $\approx$ 20 keV; it was $\approx$ 45 keV for "reconstructed" alpha particles which escaped from the front of a strip and implanted in an upstream detector so that the energies could be summed. (Uncertainties on measured values in this paper are reported at the 1σ [68%] confidence level unless specified otherwise). A multi-wire proportional counter (MWPC) was mounted upstream of the focal plane and used to distinguish implantation events from radioactive decays. The BGS fill gas was He at 0.5 torr.

Targets consisted of metallic ^{208}Pb deposited on 35 ± 5-μg/cm^2 ^{nat}C backings to a thickness of 470 ± 60 μg/cm^2. The Pb layer was covered with 5 ± 2-μg/cm^2 ^{nat}C to prevent the loss of target material caused by the beam. The isotopic composition of the Pb was 98.4% ^{208}Pb, 1.1% ^{207}Pb, and 0.5% ^{206}Pb. Nine arc-shaped target segments were mounted on the periphery of a 14-inch-diameter wheel which rotated at $\approx$ 450 rpm during the experiments to improve cooling. Before striking the target backing, the beam passed through a 45 ± 5-μg/cm^2 ^{nat}C entrance window separating the evacuated beamline from the gas-filled separator, and a negligible amount of the He fill gas.

The initial beam energy was estimated using the "Optimum Energy Rule" developed by Świątecki, Siwek-Wilczyńska, and Wilczyński [21-23]. The rule proposes that the maximum cross section in a 1*n* heavy-ion fusion-evaporation reaction is obtained when the bombarding energy is slightly greater ($\approx$ 0.3 MeV) than the sum of the evaporation residue (EVR) saddle

point mass and the neutron mass minus the masses of the projectile and target. Using masses from [24], this optimum energy was estimated to be 264.0 MeV in the laboratory frame for the ^{208}Pb(^{55}Mn, n)^{262}Bh reaction. In the initial run, 268.7-MeV $^{55}Mn^{13+}$ projectiles from the Cyclotron were chosen so that after energy losses in the entrance window, fill gas, and target backing, the lab-frame center-of-target (cot) energy E_{cot} would be 264.0 MeV. The corresponding excitation energy for compound nuclei formed at the target center was estimated to be E^*_{cot} = 14.3 MeV. Two additional projectile energies were also used: E_{cot} = 260.0 MeV (264.7 MeV from the Cyclotron, E^*_{cot} = 11.1 MeV) and E_{cot} = 268.0 MeV (272.7 MeV from the Cyclotron, E^*_{cot} = 17.4 MeV). The experimental conditions are summarized in Table I. Uncertainties in the Cyclotron projectile energies are discussed in [25] and estimated as follows. The absolute uncertainty in the projectile energies from the Cyclotron is ~1%, and the full-width-at-half-maximum (FWHM) of the energy distribution is ~0.3%. The reproducibility of Cyclotron energies in temporally separated experiments has a standard deviation of ~0.5%. The accuracy of the differences in energy between the three runs was verified by examining the linearity of the pulse heights produced by Rutherford-scattered beam particles in two *p-i-n* diode detectors versus the square of the Cyclotron frequency. Note that these uncertainties are different than the horizontal error bars shown later in Fig. 4, which represent the energy loss of projectiles in the targets. The average beam intensity throughout the experiments was approximately 150 particle nA.

At the initial E_{cot} of 264.0 MeV, the initial kinetic energy of compound nuclei formed at the target center was approximately 55 MeV. After accounting for estimated energy losses of 3 MeV in the remainder of the target, 6 MeV in 4.7 m of He at 0.5 torr, and 14 MeV in the MWPC, the implantation energy was estimated to be 32 MeV. (Energy losses in all cases were

estimated using the SRIM-2003 program [26]). Upon implantation, the large linear energy transfer of the high-*Z* EVRs creates a high density of electrons and holes in the detector. Subsequent charge recombination results in the observation of pulse heights smaller than those that would correspond to the estimated implantation energy. The observed implantation pulse heights were estimated to be 18 MeV after correcting for a pulse-height defect of $\approx$ 45% [27].

An online analysis program continually searched for the beginning of a heavy element decay chain and shut off the beam (within $\approx$ 140 μs) if one was detected. The program looked for EVRs between 12 and 25 MeV correlated to subsequent alpha decays between 8300 and 11000 keV occurring within 30.0 s. Shortly after the beginning of the experiment, the EVR energy gate was expanded to 10-25 MeV. These values allowed an implantation event followed by the decay of ^{262}Bh^{g}, ^{262}Bh^{m}, ^{261}Bh, ^{258}Db, ^{257}Db, ^{254}Lr, or ^{253}Lr to shut off the beam. The maximum vertical position difference $\Delta P_{\max}$ allowed between events was varied using the following method. The position resolution σ_{pos} of any single event with energy *E* was made dependent on the gain range used to calculate *E* [25]:

$$\sigma_{\text{pos}} = 2800E^{-1}\ \text{keV mm} + \begin{cases} 0, & \text{Low-energy range used} \\ 1.5\ \text{mm}, & \text{High-energy range used} \end{cases}. \quad (1)$$

Propagating this error in the position difference of two events ΔP gives σ_{tot}:

$$\sigma_{\text{tot}} = \sqrt{\sigma_{\text{pos},1}^2 + \sigma_{\text{pos},2}^2}\ . \quad (2)$$

The maximum position difference $\Delta P_{\max}$ was set equal to the FWHM of this distribution ($\approx 2.35\sigma_{\text{tot}}$). The beam would shut off for 180.0 s if both the energy windows and the inequality in Eq. 3 were satisfied:

$$|\Delta P| \le \Delta P_{\max} = \text{FWHM} \approx 2.35\sigma_{\text{tot}} = 2.35\sqrt{\sigma_{\text{pos},1}^2 + \sigma_{\text{pos},2}^2}\ . \quad (3)$$

The next likely alpha-decay in the chain, ^{250}Fm, formed from EC decay of ^{250}Md, has a long half-life (30 min) and was not included in the search. The total beam off time in all experiments was less than 5% of the total run time.

For EVRs with atomic number Z and velocity v, the charge states in He were estimated using Eq. 4 [25]:

$$\bar{q} = mx + b + d\sin\left\{\frac{2\pi}{32}\left[Z - (mx+b) - f\right]\right\}, \quad (4)$$

where $\bar{q}$ is the average EVR charge state, m = 0.641, b = -0.235, d = 0.517, f = 74.647, x = $(v/v_0)Z^{1/3}$, and $v_0 \approx 2.19 \times 10^6$ m/s is the Bohr velocity. The average charge state for Bh EVRs in this experiment was estimated to be +8.1. The magnetic rigidity of these EVRs was estimated to be 2.14 T m and the BGS was set accordingly.

III. RESULTS

A total of 33 decays chains originating from ^{262}Bh and 2 decay chains originating from ^{261}Bh were observed. These decay chains are shown in Figs. 1-3 in chronological order, except for the ^{261}Bh decay chains, which are shown separately in Fig. 3(b) for clarity. The individual cross sections are given in Table II along with the ^{209}Bi(^{54}Cr, n)^{262}Bh cross sections reported in [11]. The LBNL results are shown graphically in Fig. 4 together with a theoretical prediction for the ^{208}Pb(^{55}Mn, n)^{262}Bh excitation function based on calculations described in [23] for comparison purposes. Cross section error limits are computed according to methods described in [28].

The decay properties of ^{261}Bh and ^{262}Bh^m are very similar, as are those of ^{257}Db and ^{258}Db. Thus, the decay of the bohrium granddaughters ^{253}Lr and ^{254}Lr must be used to determine whether a decay chain originated from ^{261}Bh or ^{262}Bh^m. The decay properties of ^{262}Bh^g are sufficiently different from ^{261}Bh and ^{262}Bh^m that unambiguous assignments can be made when

alpha decays are observed with full energy (either stopped in the focal plane or reconstructed from focal plane and upstream signals). SF events were also useful in assigning decay chains to specific parent nuclides.

Fig. 5 shows the histogram of observed implantation pulse heights for all bohrium events. Although the implantation energy varies with initial projectile energy and EVR production location in the target, these variations are not significant relative to the width of the distribution and the data can be combined to yield improved statistics. The distribution is centered at $\approx$ 18 MeV as expected and shows a shape characteristic of ions slowed by interactions with matter. These data will be useful in planning future experiments.

Based on the horizontal positions of all bohrium EVRs, the observed average magnetic rigidity was 2.16 ± 0.03 T m (statistical uncertainty only). As with implantation energy, the magnetic rigidity varies with projectile energy and EVR production depth in the target, but again these differences are not significant. The observed rigidity corresponds to an average EVR charge state of +8.0, in good agreement with the prediction of +8.1.

The transmission of EVRs from the target to the BGS focal plane was estimated to be (65 ± 5)% for the ^{208}Pb(^{55}Mn, *n*)^{262}Bh reaction based on a Monte Carlo simulation described in [29]. Unfortunately, the vertical distribution of EVR positions was not centered at zero as expected but instead at -13 mm. This discrepancy does not appear to be due to improper equipment alignment or magnetic field inhomogeneities. Based on the observed position distribution, it was estimated that the "vertical efficiency" was (93 ± 3)%. The fraction of the horizontal EVR distribution within the focal plane was greater than 99%.

The interpretation of the decay chains was generally straightforward but some need to be discussed specifically. In chain 6, the data suggest that the EVR implanted in strip 22 very close

to the boundary with strip 21. In all three decays in that chain, some energy was also deposited in strip 21. The parent alpha lifetime of 82.9 ms identifies this event as a $^{262}Bh^{g}$ decay, even though the alpha energy is not accurately known. In chain 18, as in chain 6, some energy was also deposited in an adjacent strip. The unusually low decay energy is explained by the alpha particle passing through the strip boundary, although this energy is not recorded. Again, the long lifetime of 227 ms identifies this chain as originating from $^{262}Bh^{g}$. The ^{254}Lr event in chain 25 has an unusually large deposition energy for an escape event (6358 keV). This might be explained by the alpha particle exiting through the bottom edge of the Si layer, or traversing the strip detector at a shallow angle, exiting the strip surface with a kinetic energy of $\approx$ 2000 keV, and implanting in the small gap ($\approx$ 5 mm) which separates the face of the strip detectors from the perpendicular upstream detectors.

In the bombardment with the highest-energy projectiles (E_{cot} = 268.0 MeV), one decay chain (not shown in Figs. 1-3) was observed which was consistent with an implantation event followed by alpha decay of ^{258}Db, EC decay of ^{254}Lr, and alpha decay of ^{254}No and ^{250}Fm. The list-mode data were thoroughly searched for an event which could be attributed to the decay of ^{262}Bh but none was found. This may indicate that ^{258}Db was formed as the αn product of complete fusion, or that the decay of ^{262}Bh did not trigger a readout in the data acquisition system. Production of the αn channel is less likely than the *xn* channel because of the large barrier faced by evaporated alpha particles, even after consideration of the very favorable Q-value for alpha emission (> 10 MeV). If this decay chain is, in fact, due to the ^{208}Pb(^{55}Mn, αn)^{258}Db reaction then its cross section at E_{cot} = 268.0 MeV would be approximately 15 pb assuming a BGS transmission comparable to that for *xn* channels [30]. In contrast, if the parent nuclide in this decay chain was actually ^{262}Bh then its decay was not

recorded. No other decay chain in the current work showed these characteristics so this chain is not included in the ^{262}Bh production cross section.

IV. DISCUSSION

A. ^{262}Bh^{m} and ^{262}Bh^{g}

The existence of two alpha-decaying isomeric states in ^{262}Bh reported earlier was clearly confirmed in the current work. The half-life of all 11 decays originating from ^{262}Bh^{m} was calculated to be $9.6^{+3.6}_{-2.4}$ ms, in agreement with the half-life of 8.0 ± 2.1 ms reported by Münzenberg *et al*. (All half-lives in this paper are computed using the MLDS code [31], modified to include the covariance of all variables as described in the reference). The measured half-life of all 22 decay chains originating from ^{262}Bh^{g} is 84^{+21}_{-16} ms, a slightly more accurate value than the 102 ± 26 ms reported in [11].

There was good agreement among the alpha-particle energies observed in the current work and those reported in [11] even though some decay energies were not well-defined because the alpha-particle escaped from the front of the detector or some energy was deposited in the non-conducting region between strips. To summarize the current work: alpha groups of 10348 keV (1 event) and 10231 keV (7 events) were observed in the decay of ^{262}Bh^{m}; alpha groups of 10075 keV (5 events), 9936 keV (4 events), 9809 keV (3 events), 9727 keV (1 event), and 9657 keV (2 events) were observed in the decay of ^{262}Bh^{g}. The standard deviation of each group is $\approx$ 25 keV. The 9809-keV group (chains 2, 20, and 26) was not reported in [11] but is consistent with the ^{262}Bh decays reported in decay chains 2, 10, and 11 from Table 2 of [14], where ^{262}Bh was formed as the alpha-decay product of ^{266}Mt (Z = 109). The alpha spectra of ^{262}Bh^{g,m} observed in this experiment are shown in Fig. 6.

Decay chains 9 and 30 contained alpha particles with energies of 9655 keV and 9658 keV, respectively. These energies are not consistent with any previously reported ^{262}Bh alpha group. Both events were observed as alpha-particles fully stopped in the focal plane and so were observed with our minimum uncertainty of $\approx$ 20 keV. The good agreement of the energies suggests that incomplete charge collection from a higher energy group can be ruled out as a reason for the low observed energy. These energies are too low to be attributed to ^{261}Bh. The long observed lifetimes of 110 ms (chain 9) and 33.4 ms (chain 30) are more consistent with the decay of ^{262}Bh^{g} than ^{262}Bh^{m}, although the probability is approximately 10% that the 33.4-ms lifetime belongs to the ^{262}Bh^{m} lifetime distribution whose half-life is $9.6^{+3.6}_{-2.4}$ ms. The assignment of the new alpha group to ^{262}Bh^{g} is consistent with the fact that all previously reported ^{262}Bh^{g} alpha groups have lower energy than the known ^{262}Bh^{m} alpha groups.

Neither ^{262}Bh^{g} nor ^{262}Bh^{m} was observed to decay by SF. At the 84% confidence level, upper limit SF branches of $\leq$ 11% and $\leq$ 24% were calculated for ^{262}Bh^{g} and ^{262}Bh^{m}, respectively. These correspond to respective lower limit SF half-lives of $\geq$ 640 ms and $\geq$ 30 ms.

B. ^{261}Bh

Two decay chains (34 and 35) attributable to ^{261}Bh, the 2*n* evaporation product of complete fusion, were observed at the highest projectile energy, E_{cot} = 268.0 MeV. At this energy, the excitation energy ranges from 19.4 MeV to 15.5 MeV for compound nuclei produced at the beginning and end of the target, respectively, using masses from [24] and neglecting projectile straggling in the window, target backings, and targets. Including the kinetic energy of the two emitted neutrons, it is estimated that the first 20% of the target on the upstream side is available for production of ^{261}Bh, and similar results are obtained using masses from [32]. The observed cross section of 32^{+43}_{-21} pb (assuming constant cross section in the target) is consistent

with the expected 2*n* excitation function, and it would be informative to continue this study at higher energies to measure this excitation function.

Chain 34 can be assigned to ^{261}Bh with confidence because the high alpha energy (8671 keV) associated with the third alpha in the chain is consistent with the known ^{253}Lr^{m} alpha group with energy 8722 keV [33] but not with any known alpha group in ^{254}Lr. The assignment of chain 35 to ^{261}Bh is less certain since the alpha-particle energy of 10346 keV is consistent with either ^{261}Bh or ^{262}Bh^{m}. This alpha particle was followed 1.27 s later by a fission event, which could be explained by one of two mechanisms: either ^{261}Bh decayed to ^{257}Db which spontaneously fissioned; or ^{262}Bh^{m} decayed to ^{258}Db, which underwent EC to form the spontaneously fissioning nuclide ^{258}Rf ($t_{½}$ = 13 ± 3 ms, 100% SF [34-35]). The reported decay properties of ^{257}Db make interpretation of this decay chain even more difficult. The initial report of ^{257}Db described a single isomer with a (17 ± 11)% SF branch [36]. More recently, an additional isomer has been reported [33]. The SF branches of these isomers are ≤ 6% for ^{257}Db^{g} and ≤ 13% for ^{257}Db^{m}. Although these SF branches are small, since the observed fission lifetime is most consistent with the distribution expected for $1.50^{+0.19}_{-0.15}$-s ^{257}Db^{g} or $0.76^{+0.15}_{-0.11}$-s ^{257}Db^{m} rather than $4.4^{+0.9}_{-0.6}$-s ^{258}Db, this decay chain is assigned to ^{261}Bh with caution. However, there is a substantial probability that this decay chain originated from ^{262}Bh^{m}.

Based on two decay chains, the estimated half-life of ^{261}Bh is 10^{+14}_{-5} ms, in good agreement with $11.8^{+5.3}_{-2.8}$ ms reported by Münzenberg *et al*. [11]. The estimated ^{257}Db half-life is $0.8^{+1.1}_{-0.4}$ s, in agreement with $1.4^{+0.6}_{-0.3}$ s reported by Heßberger *et al*. [36].

C. ^{258}Db

In all 33 ^{262}Bh decay chains, the decay of ^{258}Db was observed directly via alpha decay or inferred from the decay of its fast-fissioning EC daughter ^{258}Rf. The 13 observed EC decays

resulted in a measured EC branching ratio of (39^{+11}_{-9})%, in good agreement with (33^{+9}_{-5})% reported by Heßberger *et al*. [36]. The measured half-life of all 33 decays was $4.8^{+1.0}_{-0.8}$ s, again in good agreement with $4.4^{+0.9}_{-0.6}$ s measured previously.

Heßberger *et al*. studied the direct production of ^{258}Db in the ^{209}Bi(^{50}Ti, *n*) reaction [36]. They reported that the half-life of alpha-decaying ^{258}Db ($4.4^{+0.9}_{-0.6}$ s) was one standard deviation less than that of EC-decaying ^{258}Db ($6.1^{+1.0}_{-0.8}$ s). This was attributed to the presence of an EC-decaying isomer in ^{258}Db with a half-life of 20 ± 10 s. (25 ± 5)% of all EC decays were attributed to the isomer. In the current work, the half-life of all EC-decaying ^{258}Db was $6.6^{+2.4}_{-1.6}$ s, in agreement with that reported in [36]. Unfortunately, the difference in half-lives between the alpha-decaying and EC-decaying isomers is not sufficiently large and the number of events is too small for a two-component fit to both half-lives to converge. However, if one considers only the five decays with lifetimes longer than two ^{258}Db half-lives, then a component with a half-life of $\approx$ 14 s is observed. This half-life is consistent with that proposed in [36]. In principal, one-fourth of all decay lifetimes should exceed two half-lives; in the present case this fraction is (38^{+19}_{-13})%, which differs from this figure by one standard deviation. We conclude that the current data provide supporting, but not conclusive, evidence for the existence of an EC-decaying isomer of ^{258}Db.

D. ^{258}Rf

The EC decay of 4.4-s ^{258}Db produces ^{258}Rf, which decays exclusively by SF with a short half-life of 13 ± 3 ms [34-35] and is in equilibrium with ^{258}Db. The half-life of ^{258}Rf could not be verified in the current experiment because our detectors were not sensitive to EC decay. Thus, the observed α-SF lifetimes are indicative of the lifetime of ^{258}Db and were used as

described above to investigate the proposed ^{258}Db isomer. Although fission events are clearly indicated by the large energy deposition in the focal plane ($\geq$ 140 MeV), our experiment was not suitable for measuring the total kinetic energy distribution of ^{258}Rf fission fragments.

E. ^{254}Lr

Nine full-energy alpha decays were assigned to ^{254}Lr, produced by the alpha decay of ^{258}Db. These decays could be separated into two different alpha groups with average energies of 8437 keV (2 events) and 8394 keV (7 events). These energies are consistent with those reported by Heßberger *et al*. [36]: 8460 ± 20 keV (64% intensity) and 8408 ± 20 keV (36% intensity). (Errors in alpha-group intensities were not reported). The differences in observed intensity of the alpha groups can be attributed to the low statistics in the current experiment.

The measured half-life for all 12 ^{254}Lr decays (including escape alpha events) was 22^{+9}_{-6} s, in rough agreement with the 13^{+3}_{-2} s reported in [36]. The measured branching ratios of ^{254}Lr were (60^{+11}_{-15})% alpha and (40^{+15}_{-11})% EC, consistent with (78 ± 22)% alpha and (22 ± 6)% EC reported in [36].

F. ^{254}No

The decay properties of ^{254}No have been extensively studied because of the large cross section of the ^{208}Pb(^{48}Ca, 2*n*)^{254}No reaction: 3.4 ± 0.4 μb at 227 MeV (lab-frame) [37]. The alpha-particle energy is known to be 8093 keV [9] and an improved half-life of 48 ± 3 s has recently been measured [38]. The known branching ratios are (90 ± 2)% alpha, (10 ± 2)% EC, and ($0.25^{+0.10}_{-0.06}$)% SF [39]. The 6 full-energy ^{254}No alpha decays observed in this work form a single alpha group with energy 8048 ± 30 keV, in rough agreement with the known group. The half-life of ^{254}No could not be measured in the current work because it is always formed as the

EC daughter of ^{254}Lr, for which lifetime data are not available. However, the data are consistent with a 13-s parent feeding a 48-s daughter.

G. ^{250}Md

Only one alpha decay from ^{250}Md was observed (in chain 27) among 11 total events with the remainder decaying by EC. The observed lifetime was 37.3 s, consistent with the reported half-life of 55 ± 6 s [40]. The one alpha decay was an escape event so its true energy is unknown. This single alpha event corresponds to branching ratios of (9^{+19}_{-7})% alpha and (91^{+7}_{-19})% EC. These branching ratios are in good agreement with those reported in [40]: (7 ± 3)% alpha and (94 ± 3)% EC.

H. ^{250}Fm

^{262}Bh produces ^{250}Fm via two different decay pathways: EC decay of ^{254}Lr followed by alpha decay of ^{254}No; and alpha decay of ^{254}Lr followed by EC decay of ^{250}Md. The true lifetimes are known only in those cases where ^{250}Fm was fed by the alpha decay of ^{254}No. The observed half-life of these decays is 18^{+13}_{-6} min, consistent with the known half-life of 30 ± 3 min [41]. The 16 alpha decays of ^{250}Fm form a single group with energy 7430 ± 50 keV, in excellent agreement with the reported energy of 7430 keV. The decays are also consistent with the known branch of > 90% alpha.

I. Analysis of possible random correlations

1. Expected ^{262}Bh, ^{258}Db, and ^{254}Lr random correlations

In the current work, the observed number of decay chains is small, so the possibility that these decay chains arise from random correlations of unrelated events must be considered. The requirements for a decay chain are that the events occur within appropriate energy and time gates in the same position pixel of the same strip. The methods used to calculate the expected numbers

of random correlations are described in the Appendix. ^{262}Bh, ^{258}Db, and ^{254}Lr all decay predominantly by alpha decay and are treated together. ^{250}Md is excluded from this discussion because it decays primarily by EC [(94 ± 3)% branch] to ^{250}Fm, which is treated separately in the next section. The energy range of interest was chosen to be 8300-11000 keV, large enough to cover the known alpha-particle energies of ^{262}Bh, ^{258}Db, and ^{254}Lr. In these calculations, the constant pixel size was generously chosen to be 3.0 mm, so that the number of pixels was (48 strips)(58 mm/strip)(3.0 mm/pixel)$^{-1}$ = 928. In the parlance of the Appendix, Δt_{max} was 180 s, more than ten times the half-life of ^{254}Lr, the longest-lived of the three considered nuclides. Throughout these calculations, the numbers of full-energy and reconstructed alpha decay events have been combined.

At all three beam energies, the rates of alpha decays per pixel in the energy range of interest were $\approx 10^{-6}$ s^{-1}. The probability that a single alpha decay ($n_\alpha = 1$) followed an implantation event was approximately 10^{-4} to 10^{-3} s^{-1}. Since the number of implantation events $N_{implant}$ was $\approx 10^{+4}$ in each case, the expected numbers of EVR-α correlations were large, greater than 5 at each beam energy. Yet, the expected numbers of EVR-α-α-α ($n_\alpha = 3$) correlations (for example, EVR-^{262}Bh-^{258}Db-^{254}Lr) were small, less than 10^{-6} in each case. As discussed in the Appendix, these figures represent overestimates. Thus, all alpha-decay chains are regarded as true correlations.

In the case where alpha-decay of ^{262}Bh was followed by EC of ^{258}Db and ^{258}Rf SF, the expected numbers of EVR-SF (not EVR-α-SF) correlations were estimated to be similar to the number of chain-^{250}Fm correlations as described in the next section. Once the additional requirement that an alpha-particle decay occurs between the implantation and SF events is included, the expected numbers of random EVR-α-SF correlations are decreased by four to five

orders of magnitude and are insignificant. Thus, the decay chains leading to fission of ^{258}Rf are considered real correlations.

A similar analysis was performed for the two decay chains originating from ^{261}Bh and similar results were obtained as for the ^{262}Bh decay chains.

2. Expected ^{250}Fm random correlations

As discussed previously, ^{250}Fm is frequently formed by the decay of ^{262}Bh, but the random correlation analysis for this nuclide was conducted slightly differently than for ^{262}Bh, ^{258}Db, and ^{254}Lr. ^{250}Fm has a long half-life of 30 ± 3 min so it was necessary to establish the probability that one of these ^{250}Fm-like events could randomly correlate to a *previously identified* ^{262}Bh decay chain. Using the nomenclature of the Appendix, "N_{implant}" would represent the number of decay chains which could potentially have a correlated ^{250}Fm, that is, chains which "passed through" ^{250}Fm. In this case, n_α would be fixed at one since only ^{250}Fm is under consideration.

The probability that a decay chain is correlated with a ^{250}Fm-like event is increased because of the presence of the transfer product ^{211}Po^{g} which is not completely suppressed by the BGS. The alpha-particle energy of ^{211}Po^{g} (7450.3 keV) is similar to that of ^{250}Fm (7430 keV). The total rate of alpha particles per pixel in the range 7200-7600 keV was approximately 2×10^{-6} s^{-1}. For this analysis, Δt_{max} was 7200 s. In the E_{cot} = 260.0 MeV run, no decay chains were observed which could potentially produce ^{250}Fm. In the E_{cot} = 264.0 MeV and 268.0 MeV runs, the estimated numbers of chain-^{250}Fm correlations are 0.14 and 0.12, respectively. These figures are not insignificant, even when the total numbers of decay chains that potentially passed through ^{250}Fm are considered (9 and 7, respectively). They do suggest that one or possibly two chain-^{250}Fm correlations in each run may be random. This is consistent with the fact that all

^{250}Fm events in Figs. 1-3 were observed with full energy when ≈ 20% of them should have been escape events. It is not possible to properly correlate escape events on these long time scales with the beam on, so a random correlation becomes more likely. However, these results do suggest that is possible to correlate full-energy alpha events on such time scales, provided that no interfering nuclides are present. It appears in this case that the large number of expected random chain-^{250}Fm correlations is due to the presence of ^{211}Po^{g}, not the long half-life of ^{250}Fm.

V. ^{208}Pb(^{55}Mn, n)^{262}Bh EXCITATION FUNCTION

The ^{208}Pb(^{55}Mn, n)^{262}Bh excitation function is shown in Fig. 4 along with a Gaussian fit to the data and a prediction of the "Fusion by Diffusion" theory as described in [23]. The fit shows a maximum at E_{cot} = 264.9 MeV, corresponding to E^{*}_{cot} = 15.0 MeV. This excitation energy is in good agreement with previously studied 1n excitation functions in this region (see, for example, Fig. 19 in [1]). The peak cross section in the fit is ≈ 600 pb, more than four times greater than the theoretical estimate of the maximum cross section. This may indicate the late onset of second-chance fission and that losses from fission do not become significant until the projectile energy is increased by several hundreds of keV over the expected value. According to the theory, the sticking cross section (representing approximately the probability for overcoming the Coulomb barrier) increases roughly exponentially with increasing projectile energy, so the total excitation function would increase to a higher maximum cross section before decreasing rapidly once second-chance fission becomes dominant.

A definite cross section was obtained for the ^{208}Pb(^{55}Mn, 2n)^{261}Bh reaction only at the highest projectile energy. This is consistent with the expected 2n excitation function, which should reach a maximum ≈ 8-9 MeV higher in the lab-frame and have a slightly greater width than the 1n excitation function. The maximum 2n cross section should be lower than the

maximum 1*n* cross section for reactions which are not cut off by the barrier at low projectile energies. The ^{55}Mn + ^{208}Pb reaction is expected to fall into this category.

Unexpectedly, the maximum measured cross section of 540^{+180}_{-150} pb for production of ^{262}Bh in the ^{55}Mn + ^{208}Pb reaction is much larger than that reported for the ^{54}Cr + ^{209}Bi reaction, 163 ± 34 pb (see Table I) [11]. The opposite trend would be expected based on the larger effective fissility [42] of the ^{55}Mn + ^{208}Pb system. In addition, the reported 1*n* cross section maximum in the ^{54}Cr + ^{209}Bi reaction occurred at an excitation energy of 20 ± 2 MeV, which currently would be considered an excitation energy likely to lead to production of the 2*n* product. These considerations suggest that a measurement of the complete ^{209}Bi(^{54}Cr, *n*)^{262}Bh excitation function should be performed. However, it should be noted that the experiments reported in [11] were primarily designed to confirm the discovery of bohrium [10] and were later judged to be convincing [43]. The decay properties measured for the nuclides produced are certainly valid and independent of the measurement of the detailed excitation function.

VI. SUMMARY AND CONCLUSIONS

In summary, the excitation function for production of ^{262}Bh in the odd-*Z*-projectile reaction ^{208}Pb(^{55}Mn, *n*) has been measured using the BGS at the LBNL 88-Inch Cyclotron and ^{262}Bh was positively identified. The maximum observed cross section was 540^{+180}_{-150} pb at E_{cot} = 264.0 MeV (E^{*}_{cot} = 14.3 MeV). In total, 33 decay chains of ^{262}Bh and 2 decay chains of ^{261}Bh were observed. The observed decay properties are in good agreement with previous reports [10-11]. For ^{262}Bh^{g}, a slightly improved half-life of 84^{+21}_{-16} ms was measured and a new alpha-particle group with energy 9657 keV was observed. The existence of an alpha-decaying isomer in ^{262}Bh was confirmed. No SF decay was observed in either ^{261}Bh or ^{262}Bh or in their isomeric states. The respective upper limit SF branches in ^{262}Bh^{g} and ^{262}Bh^{m} were ≤ 11% and ≤ 24%, with lower

limit SF half-lives of ≥ 640 ms and ≥ 30 ms. The large observed cross section suggests that it may be possible to perform detailed nuclear structure studies of the decay of ^{262}Bh using alpha-gamma correlation techniques. It also indicates that a complete excitation function should be measured for the production of ^{262}Bh in the ^{209}Bi(^{54}Cr, *n*) reaction in order to compare the maximum cross section values for these odd- and even-*Z*-projectile reactions.

VII. ACKNOWLEDGEMENTS

We thank D. Leitner and the staff of the LBNL 88-Inch Cyclotron for developing and delivering the intense, stable beams of ^{55}Mn. The authors wish to express their appreciation to W. J. Świątecki for many stimulating and informative discussions. This work was supported in part by the Director, Office of High Energy and Nuclear Physics, Nuclear Physics Division, United States Department of Energy and the Director, Office of Basic Energy Sciences, Chemical Sciences, Geosciences, and Biosciences Division, U.S. Department of Energy under contract number DE-AC03-76SF00098.

APPENDIX: RANDOM CORRELATION ANALYSIS METHODS

In the current work, where only a few tens of decay chains are observed, it is necessary to investigate the possibility that decay chains of interest could be replicated by random correlations of unrelated events. This section briefly details the methods used to conduct such an analysis. This discussion focuses on decay chains characterized by implantation events followed by sequential alpha-particle emission (EVR-α-α-. . .), although the same methods can be applied to EVR-SF or EVR-α-SF decay chains (or others) with appropriate modifications.

A believable decay chain occurs when events are observed which correspond to energies and decay lifetimes consistent with those expected, within reasonable distributions of positions. We wish to calculate not just the probability but the actual number of such correlations which

might occur randomly. The energy requirement is satisfied by selecting energy ranges which cover the expected alpha-particle energies of all nuclides in their respective decay chains. If these are unknown, as in the case of a search for a new element or isotope, then they have to be estimated. Let R_α be the total rate of alpha particles in the energy range. The time requirement is satisfied by selecting a maximum time $\Delta t_{\max}$ such that any observed lifetime greater than $\Delta t_{\max}$ would not be considered part of the decay chain. Typically, $\Delta t_{\max}$ is chosen to be five or six times the half-life of the longest-lived nuclide in the chain. *Note that* $\Delta t_{\max}$ *must be chosen* a priori *and cannot be influenced by the longest lifetime observed.* The position requirement is satisfied by requiring that all decays occur within a single pixel in the detector. A pixel is defined as the maximum vertical separation for which two events are considered to be in the same physical location. Implicit is the assumption that the events occur in the same strip, so that the pixel width is equal to the strip width. The total number of pixels in the focal plane is given by N_{pixel}.

In this analysis each implantation event is allowed to define a moment in time t_{implant} and a specific pixel. The number of such implantation events is N_{implant}, and a small fraction of these are true EVRs. We now wish to calculate how many alpha particles in the chosen energy range might be expected in the same pixel in the time window t_{implant} to $t_{\text{implant}} + \Delta t_{\max}$. The number of alpha particles μ expected in this time window is given by

$$\mu = (R_\alpha / N_{\text{pixel}})\Delta t_{\max} \qquad \text{(A1)}$$

if we assume the distribution of alpha particles across the focal plane is even, which is only approximately true. The probability $P(n_\alpha \mid \mu)$ of a certain number of alpha particles n_α being observed following the implantation event is given by Poisson statistics:

$$P(n_\alpha \mid \mu) = \frac{\mu^{n_\alpha}}{n_\alpha!} e^{-\mu}. \quad \text{(A2)}$$

$P(n_\alpha \mid \mu)$ is the probability that, following an implantation event, a series of random alpha decay events will exhibit a pattern indistinguishable from a true decay chain as defined by the criteria given above. The expected number of random decay chains N_{random} is then

$$N_{\text{random}} = N_{\text{implant}} \cdot P(n_\alpha \mid \mu). \quad \text{(A3)}$$

Note that the choice of n_α is affected by both objective and subjective criteria. It may depend on the alpha-particle detection efficiency and the alpha-branching ratio, and is influenced by the experimenter's choice of what constitutes a "valid decay chain." Also note that this procedure gives values of N_{random} which are overestimates. There is no requirement that the observed decay energies be consistent with previously observed data, or that they change from one nuclide to the next in a realistic way. The measured lifetimes do not have to have distributions consistent with known half-lives. In the case where n_α is less than the total number of alpha particles in the chain, there is no requirement that additional alpha particles be present to complete the chain. The addition of any of these criteria reduces the expected number of random correlations by orders of magnitude. The significance of this simple procedure lies in the fact that it depends only on quantities which are either readily measured in the experiment or chosen by the experimenter. These can then be given in published reports of relevant studies.

REFERENCES

[1] S. Hofmann, Rep. Prog. Phys. **61**, 639 (1998).

[2] S. Hofmann and G. Münzenberg, Rev. Mod. Phys. **72**, 733 (2000).

[3] S. Hofmann *et al*., Z. Phys. A **354**, 229 (1996).

[4] S. Hofmann *et al*., Eur. Phys. J. A **14**, 147 (2002).

[5] K. Morita *et al*., J. Phys. Soc. Japan **73**, 2593 (2004).

[6] Yu. Ts. Oganessian, A. G. Demin, N. A. Danilov, G. N. Flerov, M. P. Ivanov, A. S. Iljinov, N. N. Kolesnikov, B. N. Markov, V. M. Plotko, and S. P. Tretyakova, Nucl. Phys. **A273**, 505 (1976).

[7] Yu. Ts. Oganesyan, A. G. Demin, N. A. Danilov, M. P. Ivanov, A. S. Il'inov N. N. Kolesnikov, B. N. Markov, V. M. Plotko, S. P. Tret'yakova, and G. N. Flerov, Pis'ma Zh. Eksp. Teor. Fiz. **23**, 306 (1976) [JETP Lett. **23**, 277 (1976)].

[8] Yu. Ts. Oganessian *et al*., Radiochim. Acta **37**, 113 (1984).

[9] R. B. Firestone, *Table of Isotopes* (John Wiley & Sons, New York, 1996), 8th ed.

[10] G. Münzenberg, S. Hofmann, F. P. Heßberger, W. Reisdorf, K. H. Schmidt, J. H. R. Schneider, P. Armbruster, C. C. Sahm, and B. Thuma, Z. Phys. A **300**, 107 (1981).

[11] G. Münzenberg *et al*., Z. Phys. A **333**, 163 (1989).

[12] G. Münzenberg *et al*., Z. Phys. A **315**, 145 (1984).

[13] G. Münzenberg *et al*., Z. Phys. A **330**, 435 (1988).

[14] S. Hofmann, F. P. Heßberger, V. Ninov, P. Armbruster, G. Münzenberg, C. Stodel, A. G. Popeko, A. V. Yeremin, S. Saro, and M. Leino, Z. Phys. A **358**, 377 (1997).

[15] V. Ninov, K. E. Gregorich, and C. A. McGrath, in *ENAM 98: Exotic Nuclei and Atomic Masses,* edited by B. M. Sherrill, D. J. Morrissey, and C. N. Davids (American Institute of Physics, Woodbury, New York, 1998), p. 704.

[16] K. E. Gregorich and V. Ninov, J. Nucl. Radiochem. Sci. **1**, 1 (2000).

[17] C. M. Folden III, K. E. Gregorich, Ch. E. Düllmann, H. Mahmud, G. K. Pang, J. M. Schwantes, R. Sudowe, P. M. Zielinski, H. Nitsche, and D. C. Hoffman, Phys. Rev. Lett. **93**, 212702 (2004).

[18] C. M. Folden III, Ph.D. thesis, University of California, Berkeley, 2004.

[19] H. G. Essel, J. Hoffmann, N. Kurz, R. S. Mayer, W. Ott, and D. Schall, IEEE Trans. Nucl. Sci. **NS-43**, 132 (1996).

[20] H. G. Essel and N. Kurz, IEEE Trans. Nucl. Sci. **NS-47**, 337 (2000).

[21] W. J. Świątecki, K. Siwek-Wilczyńska, and J. Wilczyński, Acta Phys. Pol. B **34**, 2049 (2003).

[22] W. J. Świątecki, K. Siwek-Wilczyńska, and J. Wilczyński, Int. J. Mod. Phys. E **13**, 261 (2004).

[23] W. J. Świątecki, K. Siwek-Wilczyńska, and J. Wilczyński, Phys. Rev. C **71**, 014602 (2005).

[24] W. D. Myers and W. J. Swiatecki, Nucl. Phys. **A601**, 141 (1996); Lawrence Berkeley Laboratory Report LBL-36803, 1994 (unpublished), available at http://ie.lbl.gov/txt/ms.txt.

[25] K. E. Gregorich *et al*., Phys. Rev. C **72**, 014605 (2005).

[26] J. F. Ziegler, Nucl. Instrum. Methods Phys. Res. **B219-220**, 1027 (2004); http://www.srim.org.

[27] J. B. Moulton, J. E. Stephenson, R. P. Schmitt, and G. J. Wozniak, Nucl. Instrum. Methods **157**, 325 (1978).

[28] K.-H. Schmidt, C.-C. Sahm, K. Pielenz, and H.-G. Clerc, Z. Phys. A **316**, 19 (1984).

[29] K. E. Gregorich *et al*., Eur. Phys. J. A **18**, 633 (2003).

[30] K. E. Gregorich (private communication).

[31] K. E. Gregorich, Nucl. Instrum. Methods Phys. Res. **A302**, 135 (1991).

[32] G. Audi, A. H. Wapstra, and C. Thibault, Nucl. Phys. **A729**, 337 (2003).

[33] F. P. Heßberger *et al*., Eur. Phys. J. A **12**, 57 (2001).

[34] A. Ghiorso, M. Nurmia, J. Harris, K. Eskola, and P. Eskola, Phys. Rev. Lett. **22**, 1317 (1969).

[35] L. P. Somerville, M. J. Nurmia, J. M. Nitschke, A. Ghiorso, E. K. Hulet, and R. W. Lougheed, Phys. Rev. C **31**, 1801 (1985).

[36] F. P. Heßberger *et al*., Z. Phys. A **322**, 557 (1985).

[37] J. M. Nitschke, R. E. Leber, M. J. Nurmia, and A. Ghiorso, Nucl. Phys. **A313**, 236 (1979).

[38] M. Leino *et al*., Eur. Phys. J. A **6**, 63 (1999).

[39] A. Türler *et al*., Z. Phys. A **331**, 363 (1988).

[40] P. Eskola, Phys. Rev. C **7**, 280 (1973).

[41] S. Amiel, A. Chetham-Strode, Jr., G. R. Choppin, A. Ghiorso, B. G. Harvey, L. W. Holm, and S. G. Thompson, Phys. Rev. **106**, 553 (1957).

[42] P. Armbruster, Acta Phys. Pol. B **34**, 1825 (2003).

[43] D. H. Wilkinson, A. H. Wapstra, I. Ulehla, R. C. Barber, N. N. Greenwood, A. Hrynkiewicz, Y. P. Jeannin, M. Lefort, and M. Sakai, Pure Appl. Chem. **65**, 1757 (1993).

TABLES

TABLE I. Cross sections for the ^{209}Bi(^{54}Cr, *n*) and ^{208}Pb(^{55}Mn, *n*) reactions leading to the production of ^{262}Bh at the Gesellschaft für Schwerionenforschung (GSI) and LBNL, respectively.

Laboratory [Ref.]	Reaction	E_{cot} (MeV)	Target Thickness (mg/cm^2)	Dose (10^{16})	^{262}Bh^g + ^{262}Bh^m Cross Section (pb)
GSI	^{54}Cr + ^{209}Bi	258.9[a]	0.66	7	93^{+93}_{-50}
[11]		263.4[a]	0.39	71	163^{+34}_{-34}
		265.9[a]	0.40	18	27^{+27}_{-14}
		271.0[a]	0.40	14	< 56
LBNL	^{55}Mn + ^{208}Pb	260.0	0.47	5.7	44^{+59}_{-29}
[This work]		264.0	0.47	4.2	540^{+180}_{-150}
		268.0	0.47	7.8	210^{+80}_{-65}

[a] Estimated from data in Tables 1 and 3 in [11].

TABLE II. Cross sections for production of ^{261}Bh and ^{262}Bh as a function of E_{cot}. The numbers in parentheses are the numbers of decay chains of the given type. Upper limit cross sections are reported at the 84% confidence level so as to be comparable to upper uncertainties on measured cross sections in the rest of the table.

	E_{cot}		
Nuclide	260.0 MeV (pb)	264.0 MeV (pb)	268.0 MeV (pb)
^{261}Bh	< 41 (0)	< 56 (0)	32^{+43}_{-21} (2)
^{262}Bh^g	44^{+59}_{-29} (2)	330^{+140}_{-110} (11)	150^{+68}_{-53} (9)
^{262}Bh^m	< 41 (0)	210^{+110}_{-85} (7)	65^{+50}_{-34} (4)
Total ^{262}Bh	44^{+59}_{-29} (2)	540^{+180}_{-150} (18)	210^{+80}_{-65} (13)

FIGURE CAPTIONS

FIG. 1. ^{262}Bh decay chains observed at E_{cot} = 264.0 MeV. Information about the corresponding implantation event is given above the chain. Units are keV unless otherwise stated. The notation $x + y = z$ indicates that a signal of x keV in a strip detector was observed in coincidence with a signal of y keV in an upstream detector, with sum z keV. A black triangle in the lower right corner indicates that the beam was shut off during that event. The number of fission signals detected is indicated by the number of arrows below a nuclide. Parentheses indicate that a signal from only one end of the strip (instead of top and bottom signals) was observed and that a range of energies is possible. Brackets indicate that some energy was deposited in an adjacent strip detector, and this energy is given. These symbols also apply to Figs. 2 and 3.

FIG. 2. ^{262}Bh decay chains observed at E_{cot} = 260.0 MeV. See Fig. 1 for an explanation of symbols.

FIG. 3. Bohrium decay chains of (a) ^{262}Bh and (b) ^{261}Bh observed at E_{cot} = 268.0 MeV. See Fig. 1 for an explanation of symbols.

FIG. 4. Excitation function measured in this work for the ^{208}Pb(^{55}Mn, n)^{262}Bh reaction (diamonds). Vertical error bars represent 1σ error limits while horizontal error bars represent the range of energies covered by the projectiles as they traverse the targets. A Gaussian fit to the experimental data is shown. Squares are predictions for the ^{208}Pb(^{55}Mn, n)^{262}Bh reaction based on calculations described in [23]. Production of ^{262}Bh^{g} and ^{262}Bh^{m} has been summed.

FIG. 5. Observed pulse heights for all bohrium implantation events. These data have not been corrected for pulse-height defect.

FIG. 6. Alpha spectra observed in the decay of (a) $^{262}Bh^{m}$ and (b) $^{262}Bh^{g}$ in the current work. The average energy of each group is indicated by the arrows. Data were excluded if the energy was not known accurately because the alpha-particle escaped from the front of the detector or some energy was deposited in the non-conducting region between strips.

FIGURES

FIG. 1.

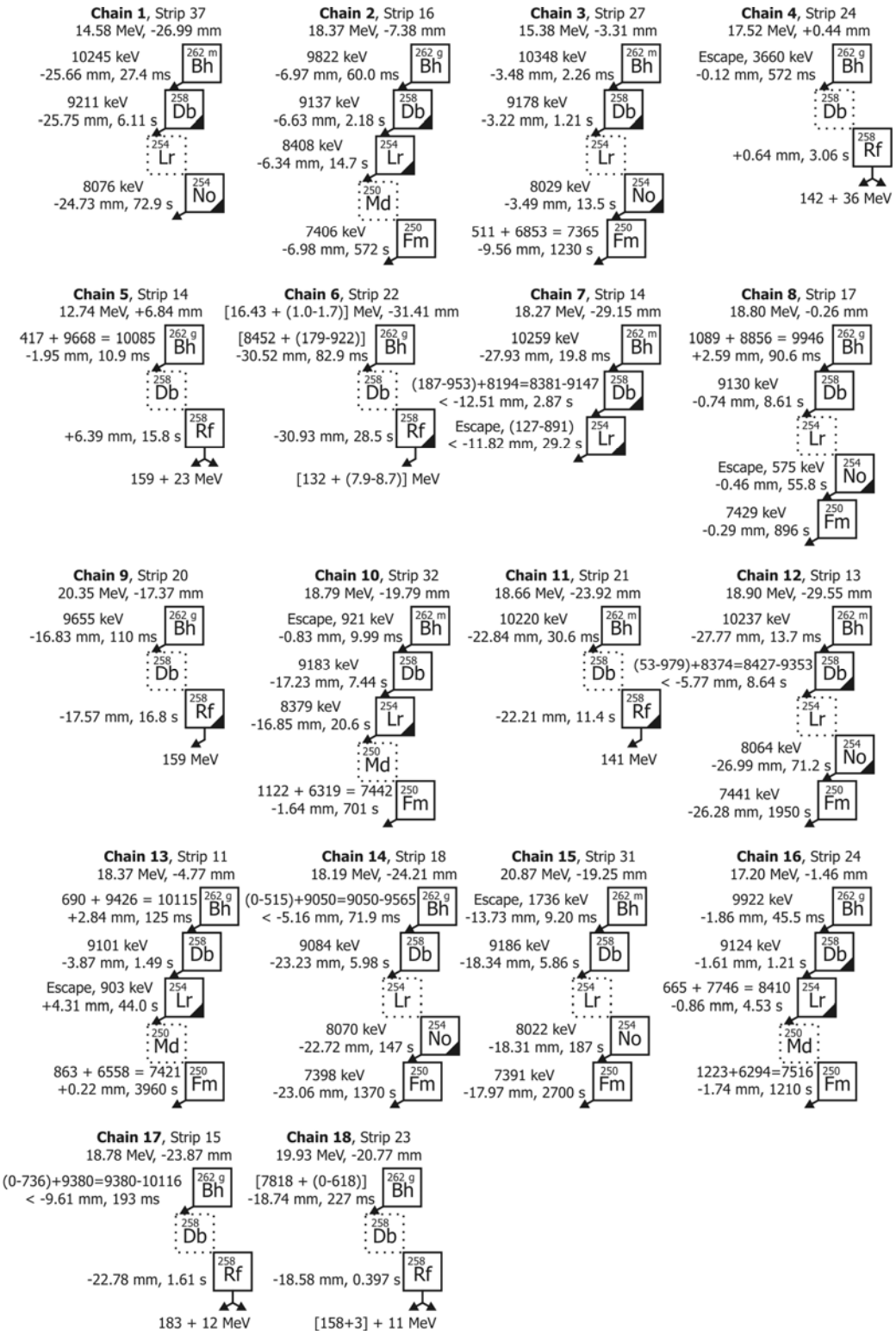

FIG. 2

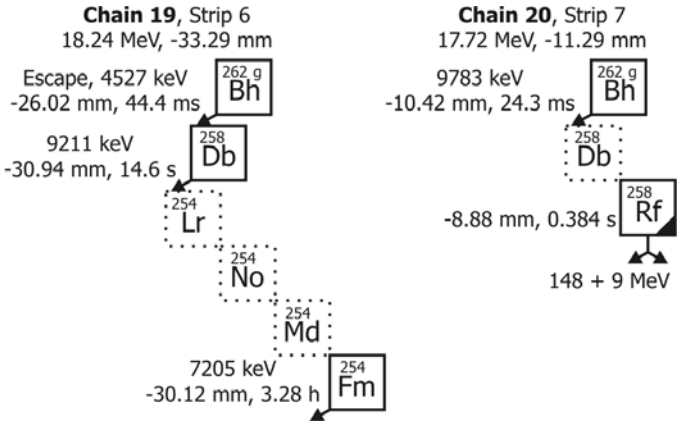
Chain 19, Strip 6
18.24 MeV, -33.29 mm
Escape, 4527 keV
-26.02 mm, 44.4 ms
262 g Bh
9211 keV
-30.94 mm, 14.6 s
258 Db
254 Lr
254 No
254 Md
7205 keV
-30.12 mm, 3.28 h
254 Fm
Chain 20, Strip 7
17.72 MeV, -11.29 mm
9783 keV
-10.42 mm, 24.3 ms
262 g Bh
258 Db
-8.88 mm, 0.384 s
258 Rf
148 + 9 MeV

FIG. 3

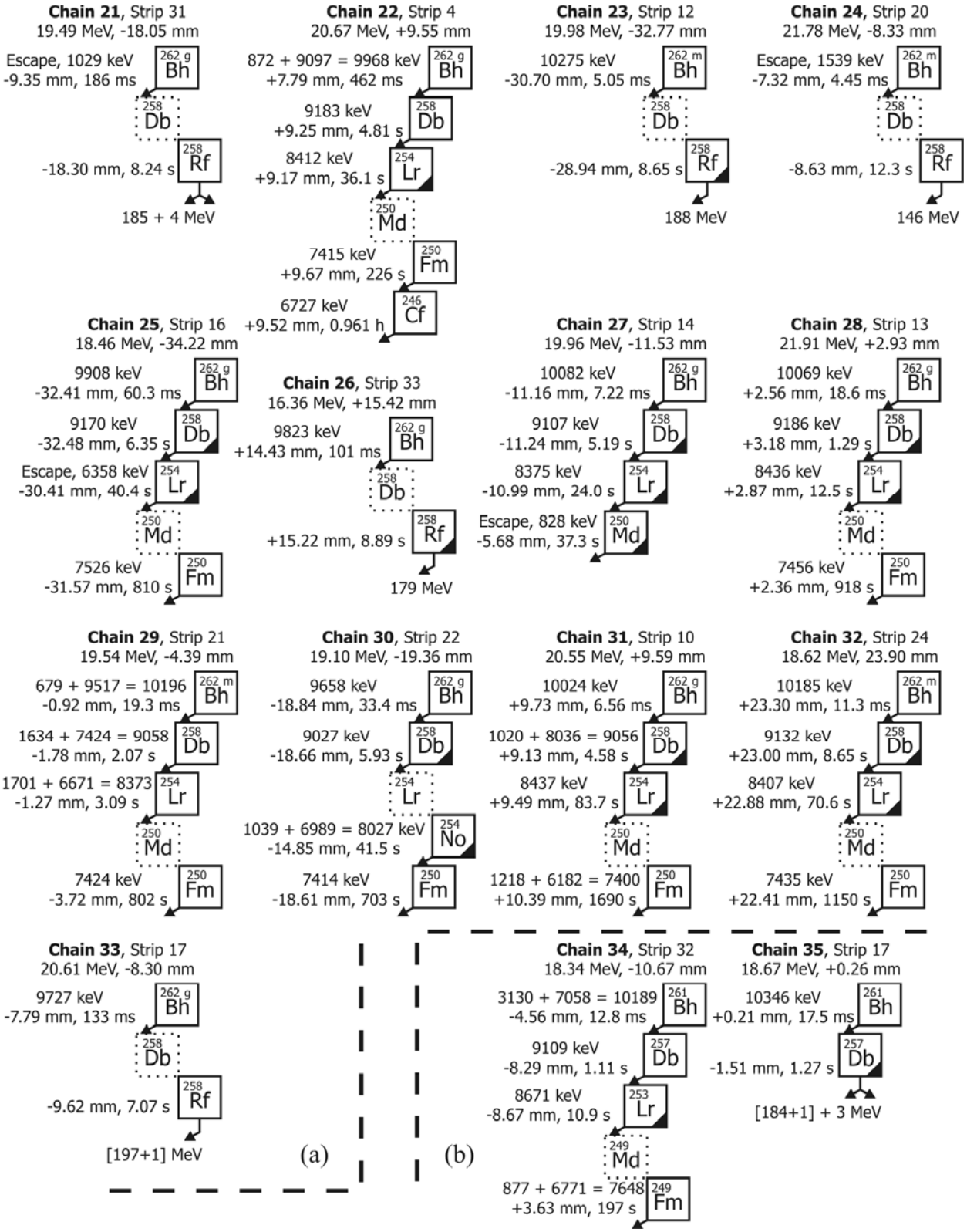
Chain 21, Strip 31
19.49 MeV, -18.05 mm
Escape, 1029 keV
-9.35 mm, 186 ms
262 g Bh
258 Db
-18.30 mm, 8.24 s
258 Rf
185 + 4 MeV
Chain 22, Strip 4
20.67 MeV, +9.55 mm
872 + 9097 = 9968 keV
+7.79 mm, 462 ms
262 g Bh
9183 keV
+9.25 mm, 4.81 s
258 Db
8412 keV
+9.17 mm, 36.1 s
254 Lr
250 Md
7415 keV
+9.67 mm, 226 s
250 Fm
6727 keV
+9.52 mm, 0.961 h
246 Cf
Chain 23, Strip 12
19.98 MeV, -32.77 mm
10275 keV
-30.70 mm, 5.05 ms
262 m Bh
258 Db
-28.94 mm, 8.65 s
258 Rf
188 MeV
Chain 24, Strip 20
21.78 MeV, -8.33 mm
Escape, 1539 keV
-7.32 mm, 4.45 ms
262 m Bh
258 Db
-8.63 mm, 12.3 s
258 Rf
146 MeV
Chain 25, Strip 16
18.46 MeV, -34.22 mm
9908 keV
-32.41 mm, 60.3 ms
262 g Bh
9170 keV
-32.48 mm, 6.35 s
258 Db
Escape, 6358 keV
-30.41 mm, 40.4 s
254 Lr
250 Md
7526 keV
-31.57 mm, 810 s
250 Fm
Chain 26, Strip 33
16.36 MeV, +15.42 mm
9823 keV
+14.43 mm, 101 ms
262 g Bh
258 Db
+15.22 mm, 8.89 s
258 Rf
179 MeV
Chain 27, Strip 14
19.96 MeV, -11.53 mm
10082 keV
-11.16 mm, 7.22 ms
262 g Bh
9107 keV
-11.24 mm, 5.19 s
258 Db
8375 keV
-10.99 mm, 24.0 s
254 Lr
Escape, 828 keV
-5.68 mm, 37.3 s
250 Md
Chain 28, Strip 13
21.91 MeV, +2.93 mm
10069 keV
+2.56 mm, 18.6 ms
262 g Bh
9186 keV
+3.18 mm, 1.29 s
258 Db
8436 keV
+2.87 mm, 12.5 s
254 Lr
250 Md
7456 keV
+2.36 mm, 918 s
250 Fm
Chain 29, Strip 21
19.54 MeV, -4.39 mm
679 + 9517 = 10196
-0.92 mm, 19.3 ms
262 m Bh
1634 + 7424 = 9058
-1.78 mm, 2.07 s
258 Db
1701 + 6671 = 8373
-1.27 mm, 3.09 s
254 Lr
250 Md
7424 keV
-3.72 mm, 802 s
250 Fm
Chain 30, Strip 22
19.10 MeV, -19.36 mm
9658 keV
-18.84 mm, 33.4 ms
262 g Bh
9027 keV
-18.66 mm, 5.93 s
258 Db
254 Lr
1039 + 6989 = 8027 keV
-14.85 mm, 41.5 s
254 No
7414 keV
-18.61 mm, 703 s
250 Fm
Chain 31, Strip 10
20.55 MeV, +9.59 mm
10024 keV
+9.73 mm, 6.56 ms
262 g Bh
1020 + 8036 = 9056
+9.13 mm, 4.58 s
258 Db
8437 keV
+9.49 mm, 83.7 s
254 Lr
250 Md
1218 + 6182 = 7400
+10.39 mm, 1690 s
250 Fm
Chain 32, Strip 24
18.62 MeV, 23.90 mm
10185 keV
+23.30 mm, 11.3 ms
262 m Bh
9132 keV
+23.00 mm, 8.65 s
258 Db
8407 keV
+22.88 mm, 70.6 s
254 Lr
250 Md
7435 keV
+22.41 mm, 1150 s
250 Fm
Chain 33, Strip 17
20.61 MeV, -8.30 mm
9727 keV
-7.79 mm, 133 ms
262 g Bh
258 Db
-9.62 mm, 7.07 s
258 Rf
[197+1] MeV
(a)
(b)
Chain 34, Strip 32
18.34 MeV, -10.67 mm
3130 + 7058 = 10189
-4.56 mm, 12.8 ms
261 Bh
9109 keV
-8.29 mm, 1.11 s
257 Db
8671 keV
-8.67 mm, 10.9 s
253 Lr
249 Md
877 + 6771 = 7648
+3.63 mm, 197 s
249 Fm
Chain 35, Strip 17
18.67 MeV, +0.26 mm
10346 keV
+0.21 mm, 17.5 ms
261 Bh
257 Db
-1.51 mm, 1.27 s
[184+1] + 3 MeV

FIG. 4

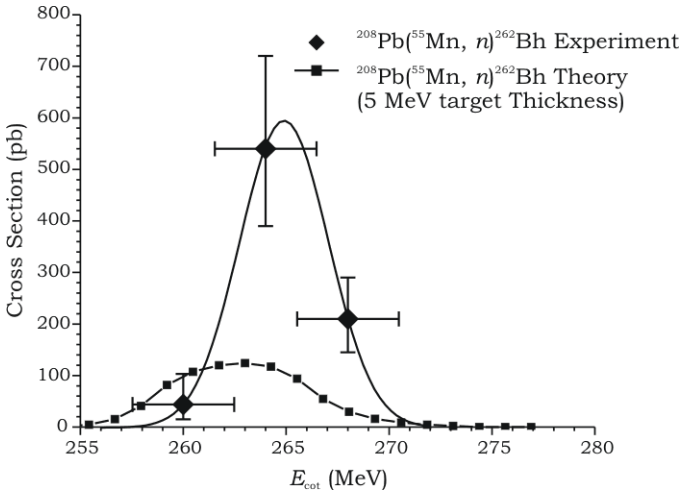
^{208}Pb(^{55}Mn, n)^{262}Bh Experiment
^{208}Pb(^{55}Mn, n)^{262}Bh Theory
(5 MeV target Thickness)
Cross Section (pb)
E_{cot} (MeV)

FIG. 5

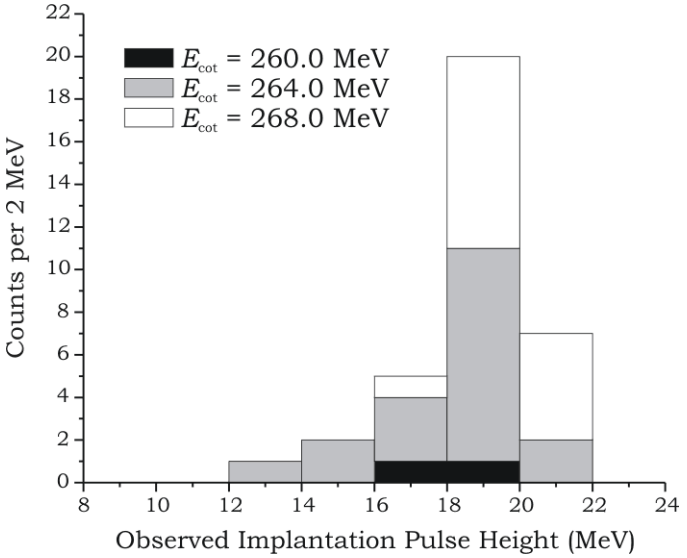
E_{cot} = 260.0 MeV
E_{cot} = 264.0 MeV
E_{cot} = 268.0 MeV
Counts per 2 MeV
Observed Implantation Pulse Height (MeV)

FIG. 6.

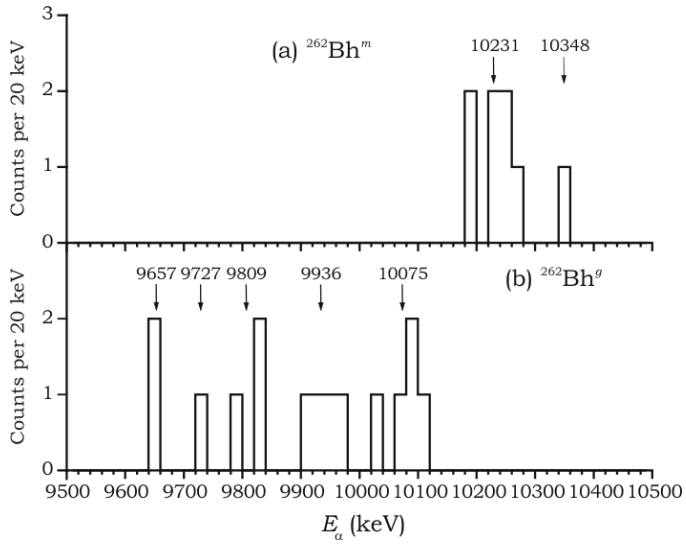
(a) $^{262}Bh^{m}$
10231
10348
Counts per 20 keV
(b) $^{262}Bh^{g}$
9657 9727 9809
9936
10075
Counts per 20 keV
9500 9600 9700 9800 9900 10000 10100 10200 10300 10400 10500
E_{α} (keV)

DISCLAIMER